

SEMICLASSICAL TWO-STEP MODEL: FURTHER DEVELOPMENTS AND APPLICATIONS

N. I. Shvetsov-Shilovski

*Institute for Theoretical Physics, Leibniz University Hanover,
Hannover, Germany*

e-mail: nikolay.shvetsov@itp.uni-hannover.de and n79@narod.ru



*30th Summer School and International Symposium on the Physics of Ionized Gases
Šabac, Serbia, August 26, 2020*

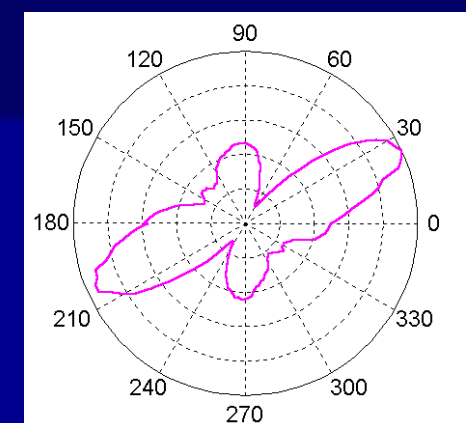
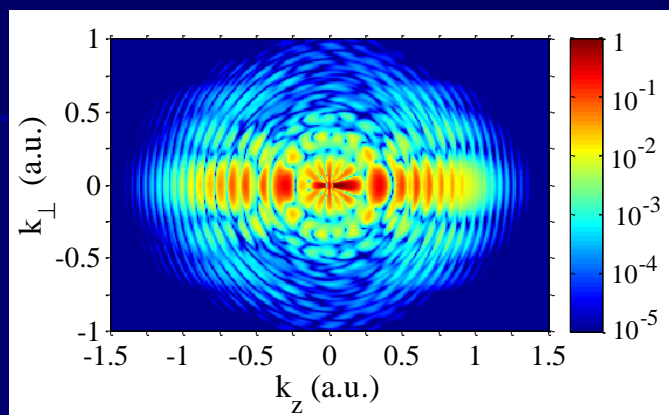
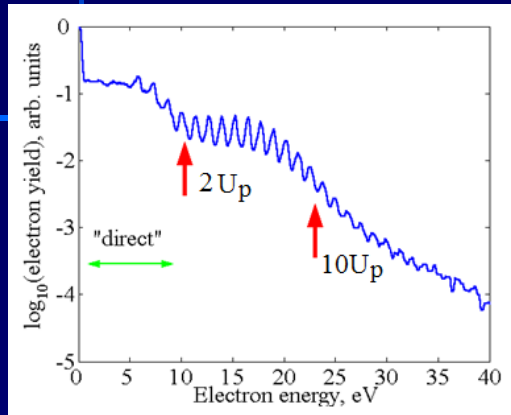
CONTENT

- Introduction. Semiclassical models
- Semiclassical two-step model (SCTS)
- Semiclassical two-step model and strong-field holography with photoelectrons
- Multielectron polarization effects: Narrowing of momentum distributions and imprints in interference structure
- Strong-field ionization of the hydrogen molecule
- Semiclassical two-step model with quantum input (SCTSQI)
- Conclusions

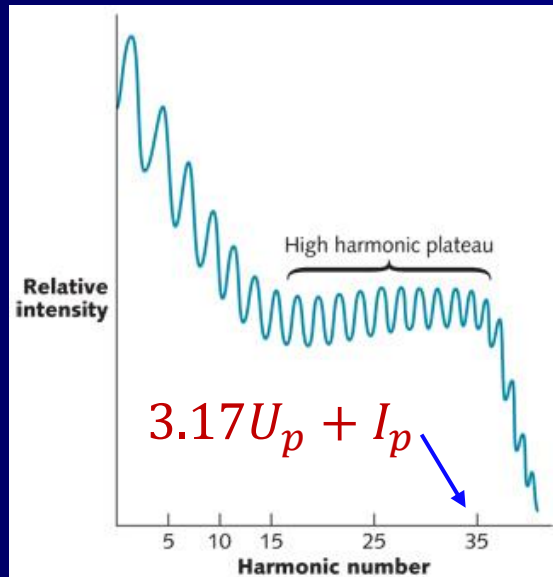
INTRODUCTION

Interaction of strong laser radiation with atoms and molecules

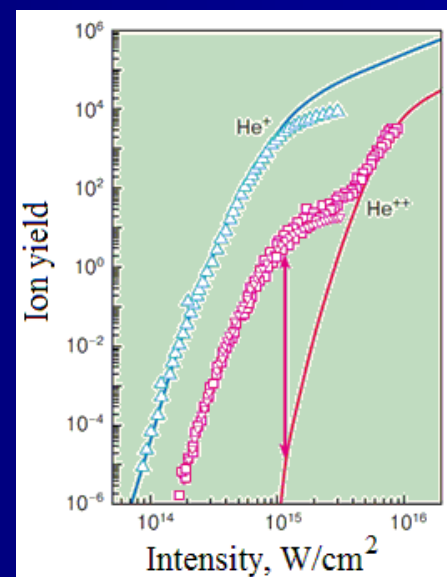
Above-threshold ionization (ATI)



High-order harmonics
generation (HHG)



Nonsequential double
ionization (NSDI)



INTRODUCTION

The main theoretical approaches of strong-field physics

- Direct numerical solution of the time-dependent Schrödinger equation (TDSE)

*M. Nurhuda and F. H. M. Faisal, Phys. Rev. A **60**, 3125 (1999)*

*H. G. Muller, Laser. Phys. **9**, 138 (1999)*

*D. Bauer and P. Koval, Comput. Phys. Commun. **174**, 396 (2006)*

- Strong-field approximation (SFA)

*L. V. Keldysh, Sov. Phys. JETP **20**, 1307 (1965)*

*F. H. M. Faisal, J. Phys. B **6**, L89 (1973)*

*H. R. Reiss, Phys. Rev A **22**, 1786 (1980)*

Coulomb-corrected strong-field approximation (CCSFA)

*S. V. Popruzhenko and D. Bauer, J. Mod. Opt. **55**, 2573 (2008)*

*T.-M. Yan, S. V. Popruzhenko, M. J. J. Vrakking, and D. Bauer, Phys. Rev. Lett. **105**, 253002 (2010)*

Eikonal-Volkov approximation (EVA) and the analytical R-matrix (ARM) method

*O. Smirnova, M. Spanner, and M. Ivanov, Phys. Rev. A **77**, 033407 (2008)*

*L. Torlina and O. Smirnova, Phys. Rev. A **86**, 043408 (2012)*

Coulomb quantum orbit strong-field approximation (CQSFA)

*X. Y. Lai, C. Poli, H. Schomerus, and C. Faria, Phys. Rev. A **92**, 043407 (2015)*

- Semiclassical models

H. B. van Linden van den Heuvell and H. G. Muller in Multiphoton processes (1988)

*T. F. Gallagher, Phys. Rev. Lett. **61**, 2304 (1988)*

*P. B. Corkum, N. H. Burnett, and F. Brunel, Phys. Rev. Lett. **62**, 1259 (1989)*

*P. B Corkum, Phys. Rev. Lett. **71**, 1994 (1993)*

SEMICLASSICAL MODELS

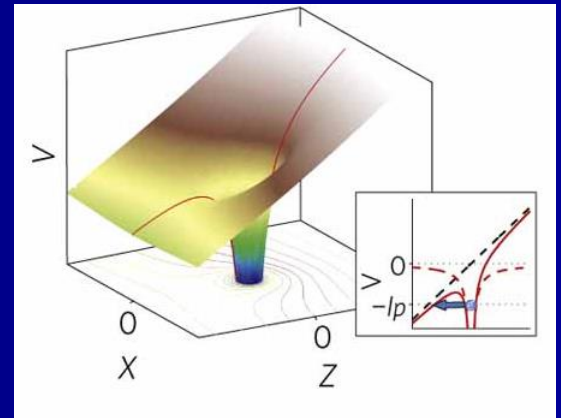
Semiclassical model for strong-field ionization

$$\boxed{\frac{d^2\vec{r}}{dt^2} = -\vec{F}(t) - \nabla V}$$

- Starting point of the electron trajectory
- Initial velocity

$$V(r) = -\frac{Z}{r} \quad \left(-\frac{1}{2}\Delta - \frac{Z}{r} + \vec{F} \cdot \vec{r} \right) \Psi = -I_p \Psi$$

$$-\frac{\beta_2}{2\eta} + \frac{m^2 - 1}{8\eta} - \frac{F\eta}{8} = -\frac{I_p}{4}$$

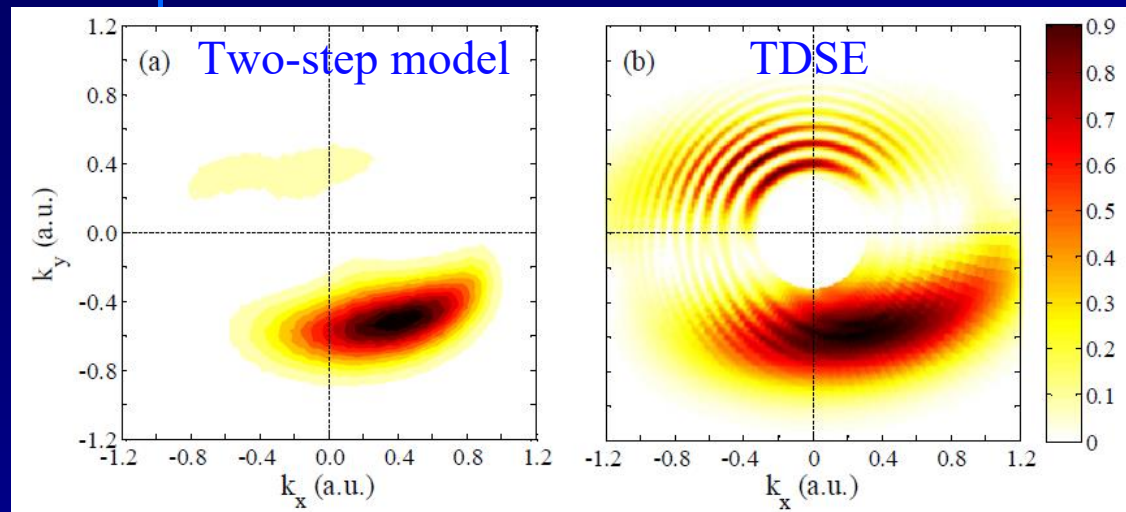


$$w(t_0, v_{0\perp}) \sim \exp\left(-\frac{2\kappa^3}{3F(t_0)}\right) \exp\left(-\frac{\kappa v_{0\perp}^2}{F(t_0)}\right) \quad v_{0\parallel} = 0 \quad \kappa = (2I_p)^{1/2}$$

$$\begin{aligned} \vec{r} &= \vec{r}(t_0, v_{0\perp}, t_f) & \frac{q^2}{2} - \frac{Z}{r} &= \frac{p^2}{2} & \vec{p} &= p \frac{\vec{L} \times \vec{A}}{1 + p^2 L^2} & \text{binning} \\ \vec{q} &= \vec{q}(t_0, v_{0\perp}, t_f) & \end{aligned}$$

SEMICLASSICAL MODELS

- Semiclassical simulations can help to identify **in terms of classical trajectories** the specific mechanism underlying the strong-field phenomena of interest.
- Semiclassical simulations are usually computationally **much simpler** than the direct numerical solution of the TDSE. There are some strong-field problems, for which semiclassical models are **the only** feasible approach.



Semiclassical models have not been able to describe quantum interference

*Modified from Fig. 2. in
N.I. Shvetsov-Shilovski,
D. Dimitrovski, and L. B. Madsen,
Phys. Rev. A 87, 013427 (2013)*

- G. van de Sand and J. M. Rost, *Phys. Rev. A* **62**, 053403 (2000)
- Quantum trajectory Monte-Carlo (QTMC)
M. Li, J.-W. Geng, H. Liu et al., *Phys. Rev. Lett.* **112**, 113002 (2014)
- Coulomb quantum orbit strong-field approximation (CQSFA)
X.-Y. Lai, C. Poli, H. Schomerus, and C. Faria, *Phys. Rev. A* **92**, 043407 (2015)
- Semiclassical two-step model (SCTS)
N. I. Shvetsov-Shilovski, M. Lein, L. B. Madsen, E. Räsänen, C. Lemell, J. Burgdörfer, D. Arbó, and K. Tökési, *Phys Rev. A*, **94**, 013415 (2016)

SEMICLASSICAL TWO-STEP MODEL (SCTS)

Phase in the QTMC

The Coulomb potential is considered in the first order perturbation theory:

$$S(t_0, v_0) = \int_{t_0}^{\infty} \left[\frac{v^2(t)}{2} - \frac{1}{r(t)} + I_p \right] dt \quad "1/r" \text{ phase}$$

Phase in the SCTS

SCTS accounts for the ionic potential **beyond the semiclassical perturbation theory**:

$$S(p_1, p_2) = \int_{t_0}^{t_1} dt \{ -q(t)\dot{p}(t) - H[p(t)q(t)] \}$$

W. H. Miller, *Adv. in Chem. Phys.*, **25**, 69 (1971)
K. G. Kay, *Annu. Rev. Phys. Chem.*, **56**, 255 (2005)

$$U = \vec{E}(t)\vec{r} - \frac{1}{r}$$
$$\frac{d\vec{v}}{dt} = -\vec{E}(t) - \frac{\vec{r}}{r^3}$$

$$H = T + U = \frac{v^2}{2} + \vec{E}(t)\vec{r} - \frac{1}{r}$$

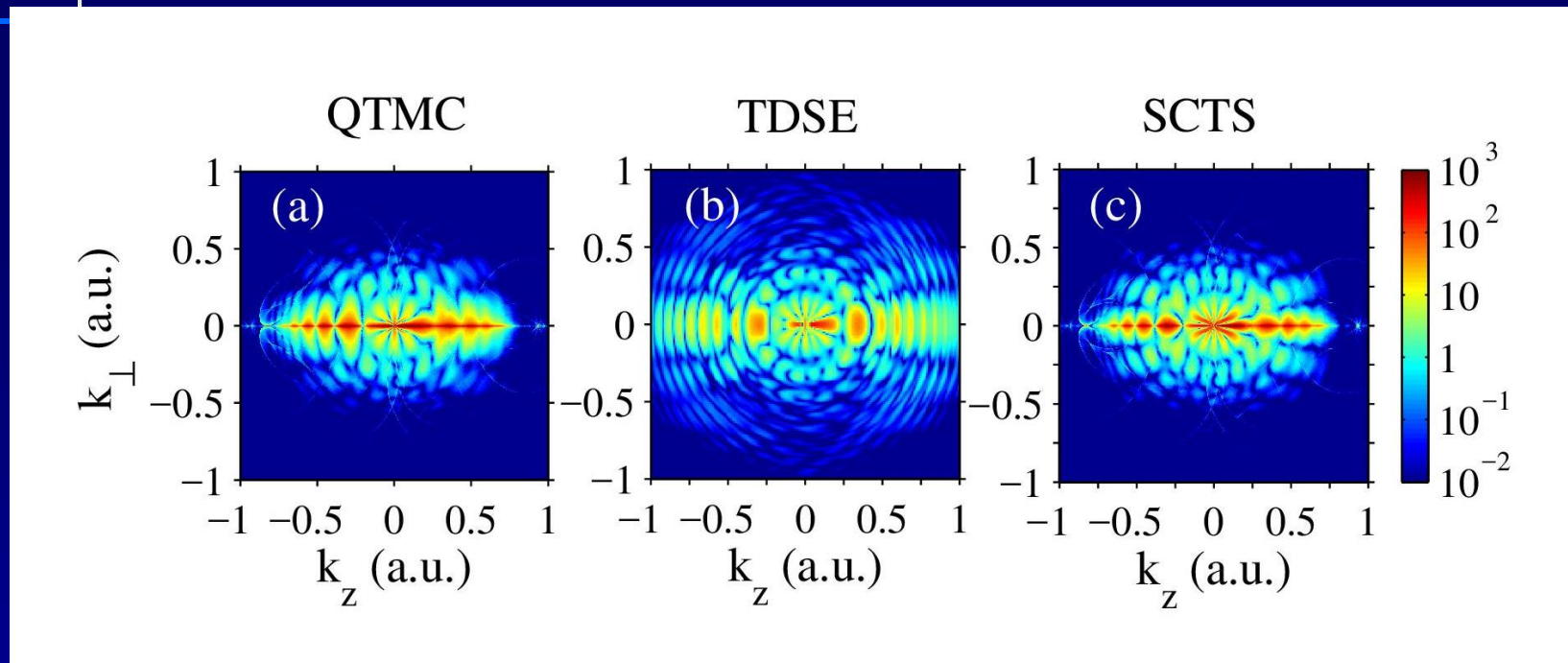
$$S(t_0, v_0) = \int_{t_0}^{\infty} \left[\frac{v^2(t)}{2} - \frac{2}{r(t)} + I_p \right] dt \quad "2/r" \text{ phase}$$

$$\frac{dR}{d^3 k} = \left| \sum_{j=1}^{n_p} \exp \left[iS(t_0^j, \vec{v}_0^j) \right] \right|^2$$

COMPARISON WITH THE TDSE

$$\vec{A}(t) = \frac{F}{\omega} \sin^2 \left(\frac{\omega t}{2n} \right) \sin(\omega t + \varphi) \vec{e}_z$$

H, 800 nm, 0.9×10^{14} W/cm², 3 cycles

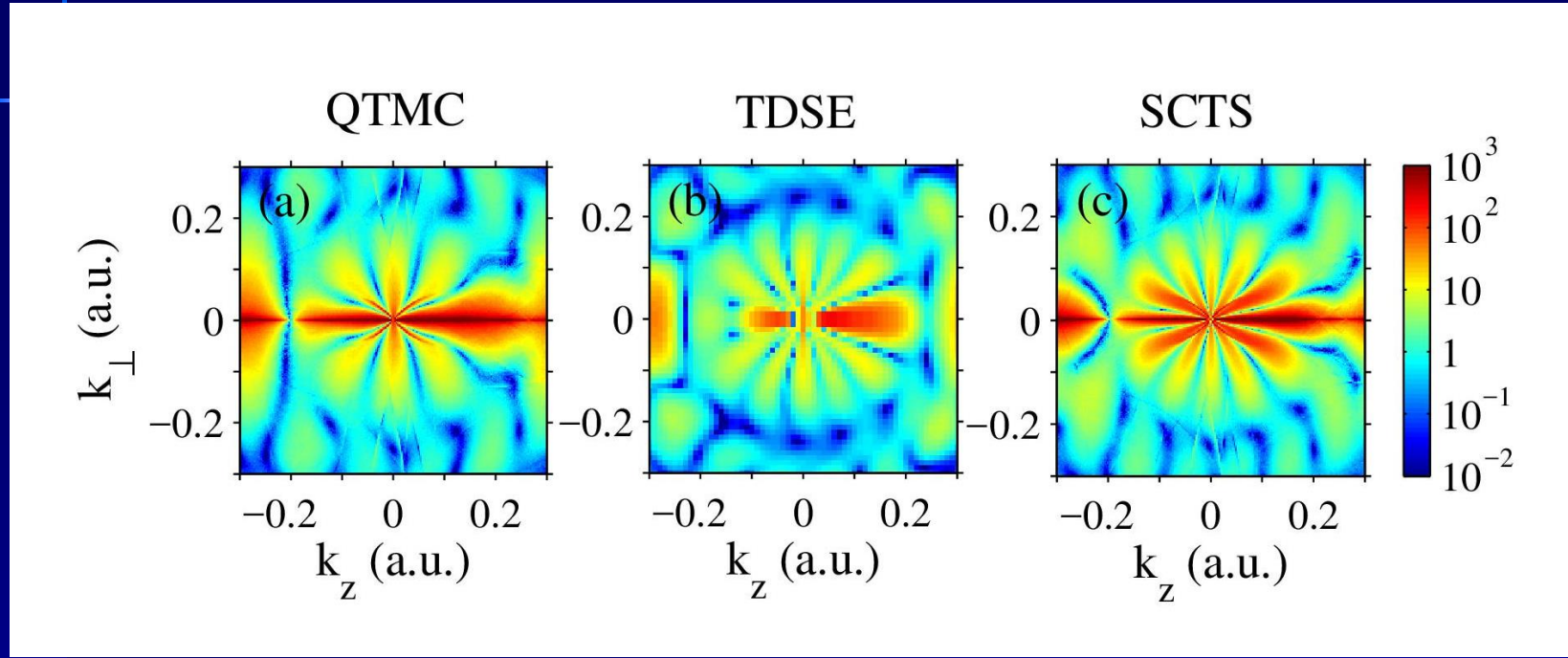


The distributions are normalized to the peak value. A logarithmic color scale is used. The laser field is linearly polarized along the z axis.

Modified from Fig. 1 in N. I. Shvetsov-Shilovski, M. Lein, L. B. Madsen, E. Räsänen, C. Lemell, J. Burgdörfer, D. Arbó, and K. Tőkési, Phys Rev. A, **94**, 013415 (2016)

COMPARISON WITH THE TDSE

$$\vec{A}(t) = \frac{F_0}{\omega} \sin^2 \left(\frac{\omega t}{2n} \right) \sin(\omega t + \varphi) \vec{e}_z$$



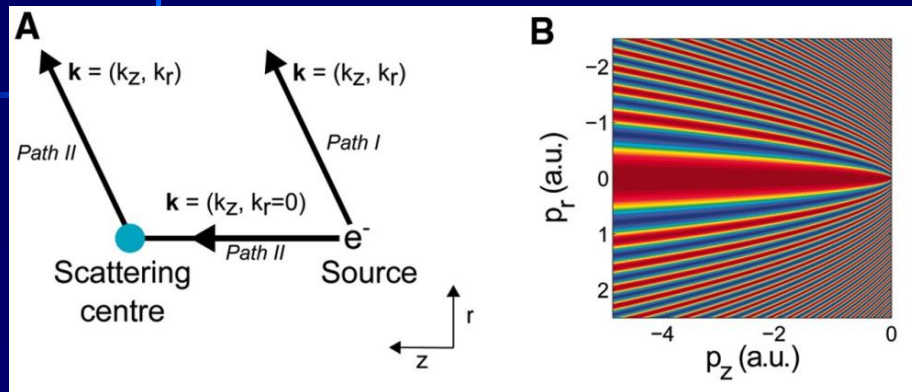
Magnification for $|k_z|, |k_{\perp}| < 0.3$. a.u.

While the SCTS closely matches the nodal pattern of the TDSE, the QTMC model yields fewer nodal lines, which is a direct consequence of the underestimate of the Coulomb interaction in the QTMC treatment of the interference phase.

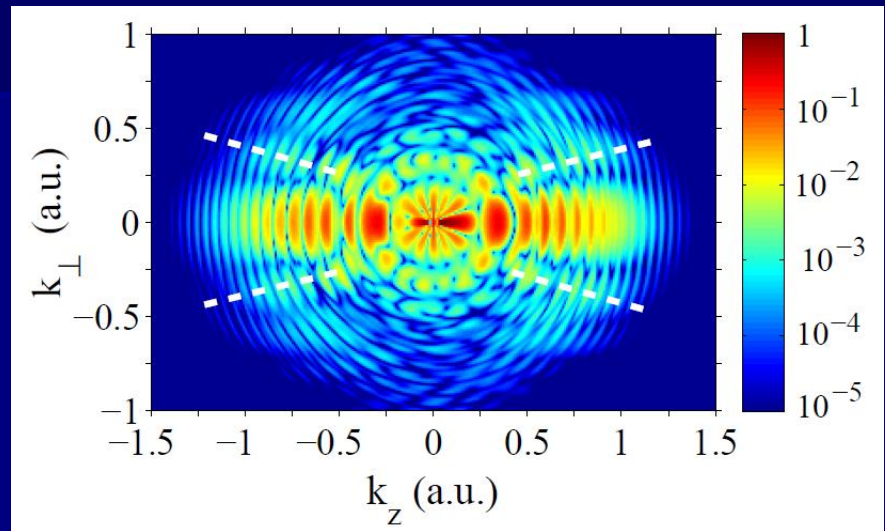
Modified from Fig. 2 in N. I. Shvetsov-Shilovski, M. Lein, L. B. Madsen, E. Räsänen, C. Lemell, J. Burgdörfer, D. Arbó, and K. Tókési, Phys Rev. A, 94, 013415 (2016)

SEMICLASSICAL TWO-STEP MODEL AND STRONG-FIELD HOLOGRAPHY WITH PHOTOELECTRONS

H , 800 nm, $0.9 \times 10^{14} \text{ W/cm}^2$, 8 cycles



Modified from Fig. 1 in
Y. Huismans et al., *Science* **331**, 61 (2011)



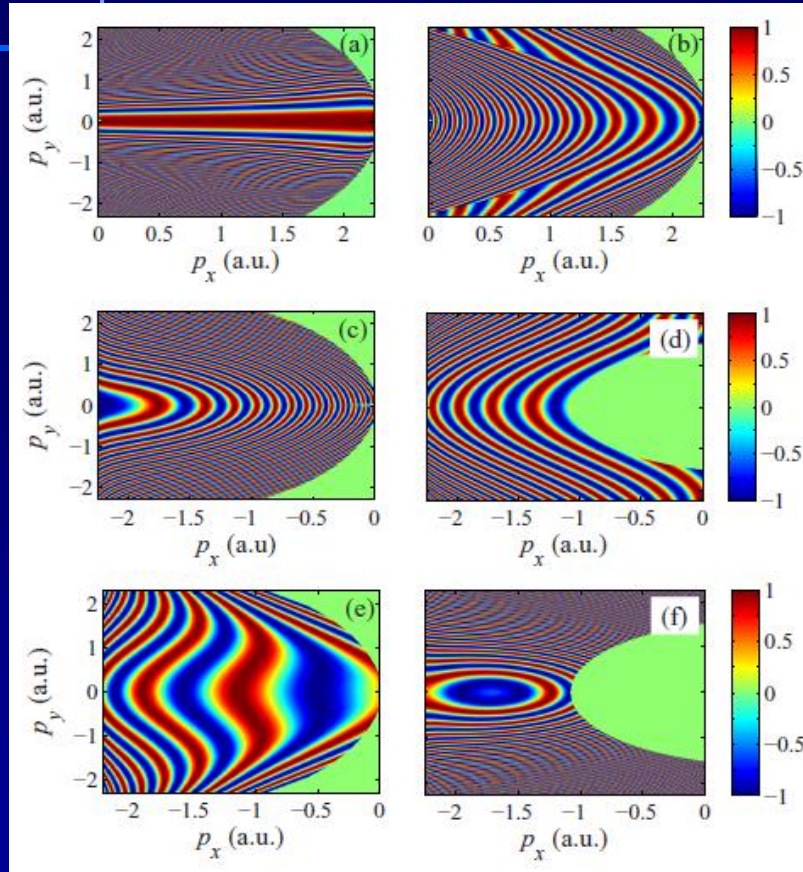
Strong-field holography with photoelectrons has several important advantages:

- The method can be realized in a table-top experiment.
- The hologram encodes temporal and spatial information not only about the ion, but about the recolliding electron as well.
- Attosecond time resolution can be achieved for the photoelectron dynamics.

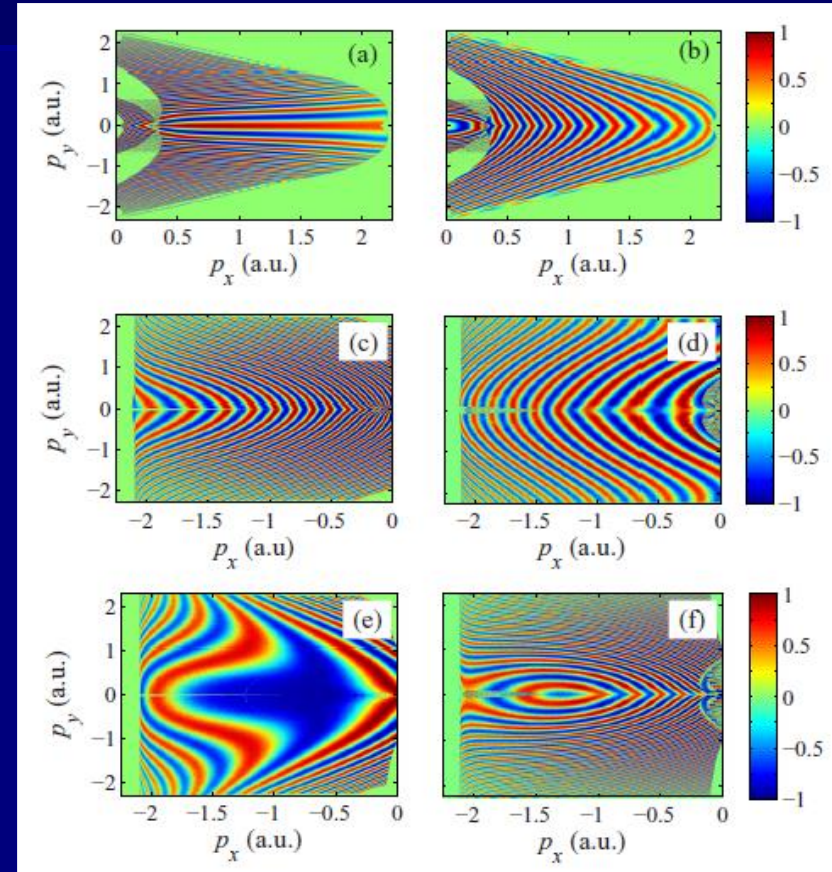
SEMICLASSICAL TWO-STEP MODEL AND STRONG-FIELD HOLOGRAPHY WITH PHOTOELECTRONS

H , 800 nm, 6.0×10^{14} W/cm²

Three-step model (no Coulomb)



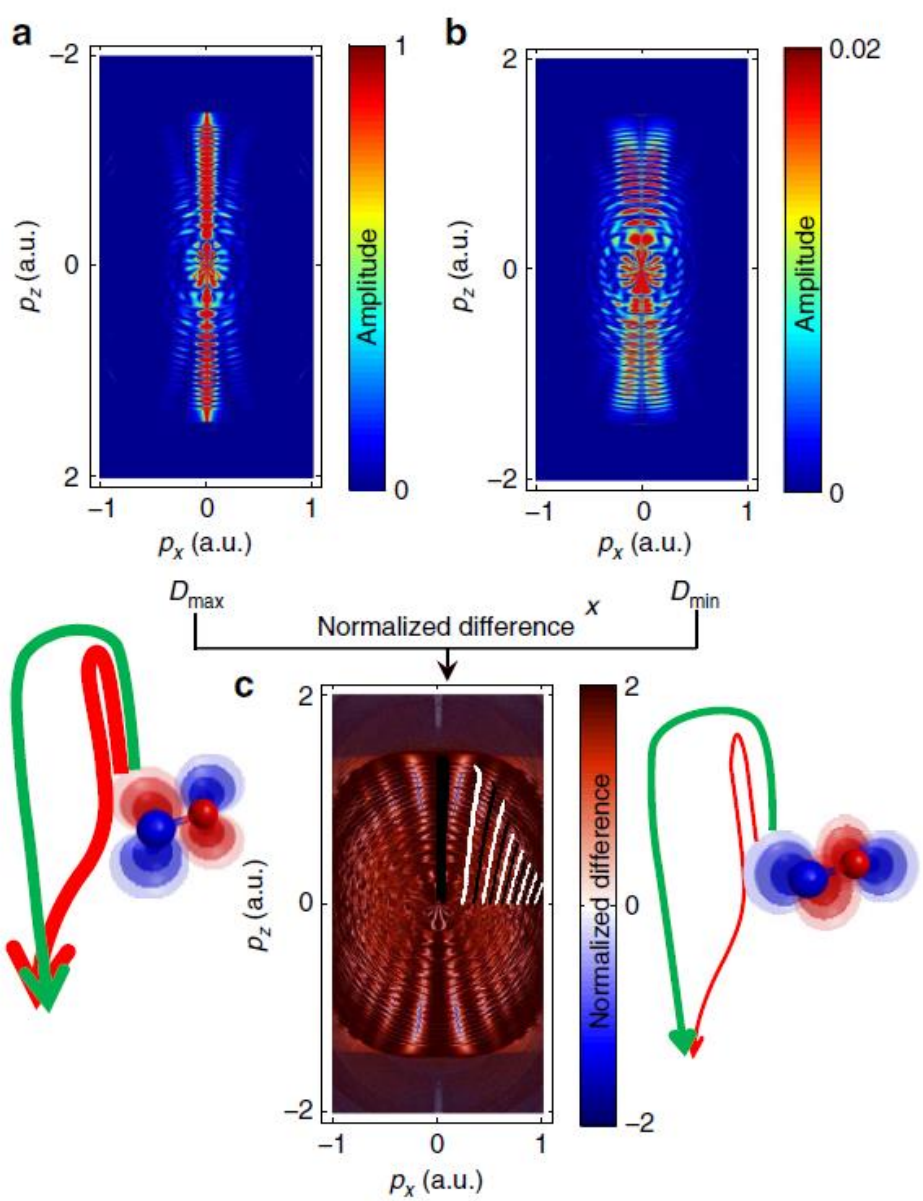
SCTS



The Coulomb potential modifies the interference patterns significantly

N. I. Shvetsov-Shilovski and M. Lein, Phys. Rev. A 97, 013411 (2018)

SEMICLASSICAL TWO-STEP MODEL AND STRONG-FIELD HOLOGRAPHY WITH PHOTOELECTRONS



NO, 800 nm, $2.4 \times 10^{14} \text{ W/cm}^2$, 35 fs

S. G. Walt, N. Bhargava Ram, M. Atala, N. I. Shvetsov-Shilovski, A. von Conta, D. Baykusheva, M. Lein, and H. J. Wörner, Nat. Commun. 8, 15651 (2017)

$$S(t_0, v_{0\perp}) = \int_{t_0}^{\infty} \left[\frac{v^2(t)}{2} - \frac{2}{r(t)} + I_p \right] dt$$

MULTELECTRON POLARIZATION EFFECTS

The theoretical models capable to account for multielectron (ME) effects in strong-field processes:

- Time-dependent density-functional theory
E. Runge and E. K. U. Gross, Phys. Rev. Lett. 52, 997 (1984)
C. A. Ullrich (Oxford University Press, Oxford, 2012)
- Multiconfiguration time-dependent Hartree-Fock theory
J. Zanghellini, M. Kitzler, T. Brabec and A. Scrinzi, J. Phys. B. 37, 763 (2004)
J. Caillat, J. Zanghellini, M. Kitzler et al., Phys. Rev. A 71, 012712 (2012)
- Time-dependent restricted-active-space and time-dependent complete-active-space self-consistent-field theory
H. Miyagi and L. B. Madsen, Phys. Rev. A 87, 062511 (2013)
T. Sato and K. L. Ishikawa, Phys. Rev. A 88, 023402 (2013)
- Time-dependent *R*-matrix theory
P. G. Burke and V. M. Burke, J. Phys. B 30 L383 (1997)
M. A. Lysaght, H. W. van der Hart, and P. G. Burke, Phys. Rev. A 79, 053411 (2009)
- *R*-matrix method with time-dependence
L. A. A. Nikolopoulos, J. S. Parker, and K. T. Taylor, Phys. Rev. A 78, 063420 (2008)
L. R. Moore, M. A. Lysaght, L. A. A. Nikolopoulos et al., J. Mod. Opt. 58, 1132 (2011)

MULTELECTRON POLARIZATION EFFECTS

- Time-dependent analytical *R*-matrix theory

L. Tirlina and O. Smirnova, Phys. Rev. A **86**, 043408 (2012)

- Semiclassical models

A. N. Pfeiffer, C. Cirelli, M. Smolarski et al, Nat. Phys. **8**, 76 (2012)

N.I. Shvetsov-Shilovski, D. Dimitrovski, and L. B. Madsen, Phys. Rev. A **85**, 023428 (2012)

D. Dimitrovski, J. Maurer, H. Stapelfeldt, and L. B. Madsen,

Phys. Rev. Lett. **113**, 103005 (2014)

H.-P. Kang, S.-P. Su, Y.-L. Wang et al., J. Phys. B **51**, 105601 (2018)

Laser-induced polarization of the ionic core

$$V(\vec{r}, t) = -\frac{Z}{r} - \frac{\alpha_I \vec{F}(t) \cdot \vec{r}}{r^3}$$

T. Brabec, M. Côté, P. Boulanger, and L. Ramunno, Phys. Rev. Lett. **95**, 073001 (2005)

Z. X. Zhao and T. Brabec, J. Mod. Opt. **54**, 981 (2007)

D. Dimitrovski, C. P. J. Martiny, and L. B. Madsen, Phys. Rev. A **82**, 053404 (2010)

Tunnel Ionization in Parabolic coordinates with Induced dipole and Stark shift (TIPIS)

A. Pfeiffer, C. Cirelli, M. Smolarski, et al., Nat. Phys. **8**, 76 (2012)

MULTELECTRON POLARIZATION EFFECTS

For different atoms and molecules the photoelectron momentum distributions are highly sensitive to ME effects as captured by the induced dipole of the atomic core.

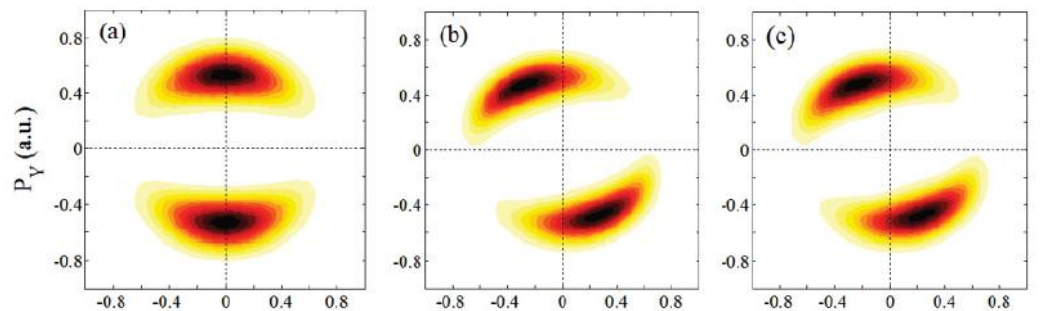
Two-step

Coulomb

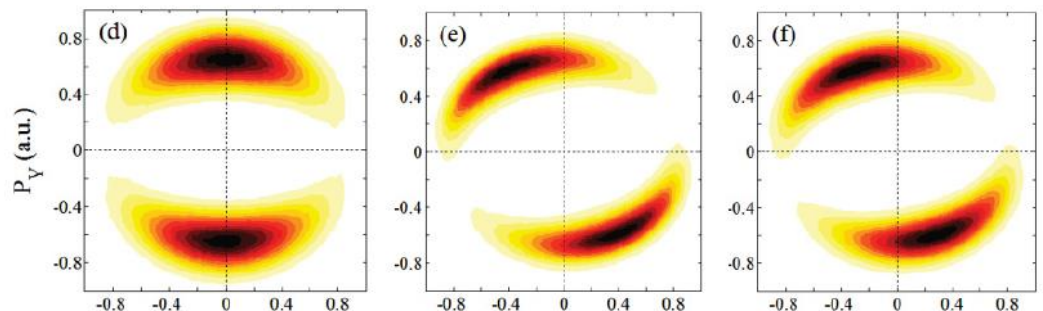
TIPIS

Mg, 1600 nm, 8 cycles, ellipticity=0.78

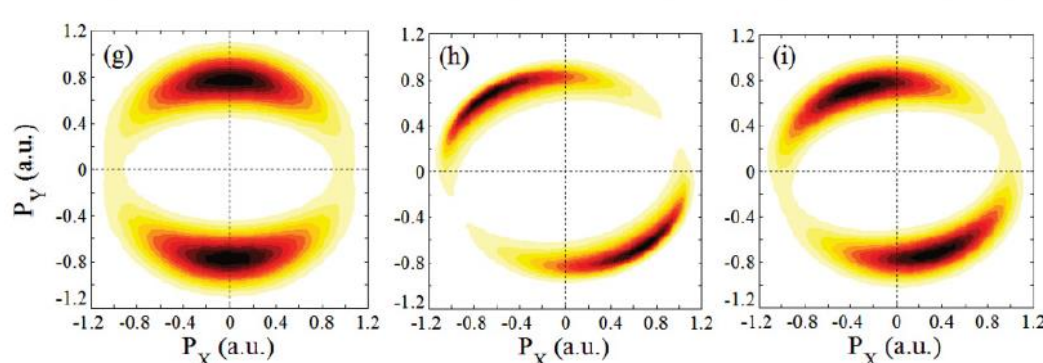
$2.35 \times 10^{13} \text{ W/cm}^2$



$3.5 \times 10^{13} \text{ W/cm}^2$



$5.0 \times 10^{13} \text{ W/cm}^2$



*Modified from Fig. 3 in
N. I. Shvetsov-Shilovski, D. Dimitrovski,
and L. B. Madsen, Phys. Rev. A 85,
023428 (2012)*

MULTELECTRON POLARIZATION EFFECTS

Combination of the SCTS with the TIPIS model

$$S(t_0, v_{0,\perp}) = \int_{t_0}^{\infty} dt \{ -\vec{r}(t) \dot{\vec{p}}(t) - H[\vec{r}(t), \vec{p}(t)] \}$$

W. H. Miller, *Adv. in Chem. Phys.*, **25**, 69 (1971)
K.G. Kay, *Annu. Rev. Phys. Chem.*, **56**, 255 (2005)

For an arbitrary effective potential $V(\vec{r}, t)$

$$S(\vec{r}, t) = -\vec{v}_o \cdot \vec{r}(t_0) + I_p t_0 - \int_{t_0}^{\infty} dt \left\{ \frac{p^2(t)}{2} - V[\vec{r}(t)] - \vec{r}(t) \cdot \vec{\nabla}V[\vec{r}(t)] \right\}$$

$$V(\vec{r}, t) = -\frac{Z}{r} - \frac{\alpha_I \vec{F}(t) \cdot \vec{r}}{r^3}$$

$$S(\vec{r}, t) = -\vec{v}_o \cdot \vec{r}(t_0) + I_p t_0 - \int_{t_0}^{\infty} dt \left\{ \frac{p^2(t)}{2} - \frac{2Z}{r} - \frac{3\alpha_I \vec{F}(t) \cdot \vec{r}}{r^3} \right\}$$

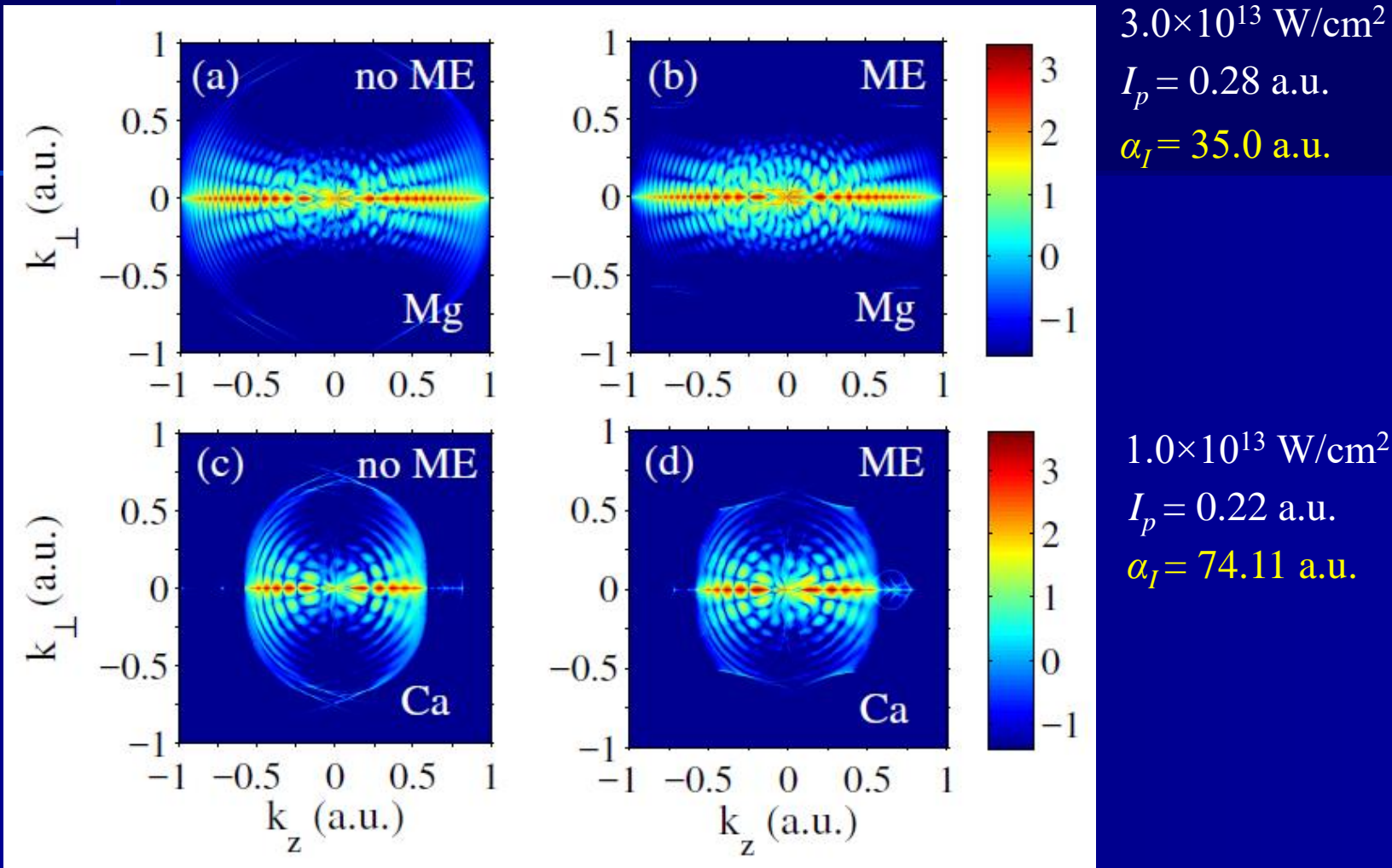
"2/r" phase

ME term

$$\frac{dR}{d^3k} = \left| \sum_{j=1}^{n_p} \exp \left[i\Phi(t_0^j, \vec{v}_0^j) \right] \right|^2$$

MULTELECTRON POLARIZATION EFFECTS

1600 nm, 8 cycles



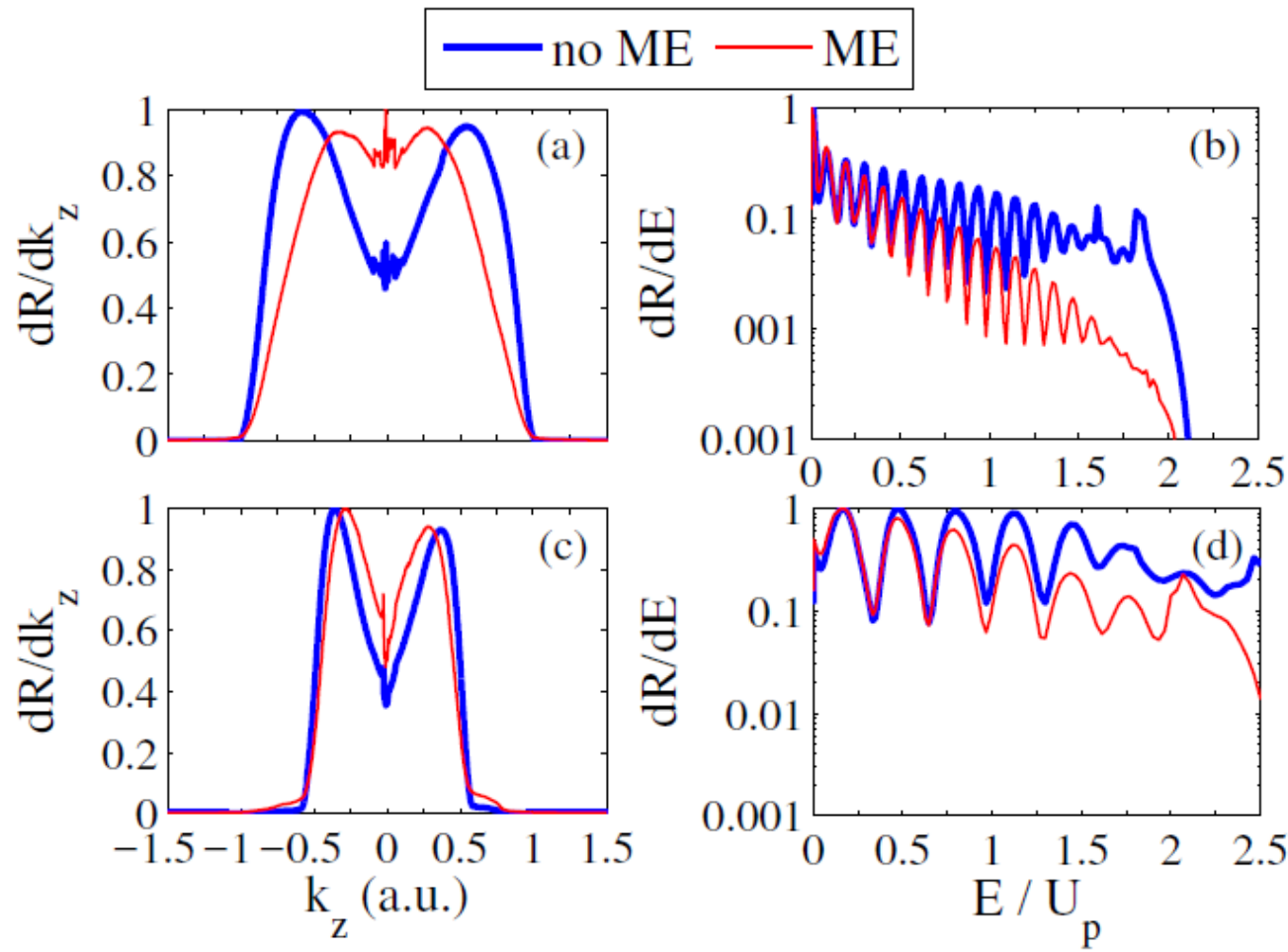
The presence of the ME term leads to two different effects:

- *Narrowing of the longitudinal momentum distributions*
- *Modification of the interference patterns*

MULTELECTRON POLARIZATION EFFECTS

Narrowing of the longitudinal momentum distributions

1600 nm, 8 cycles



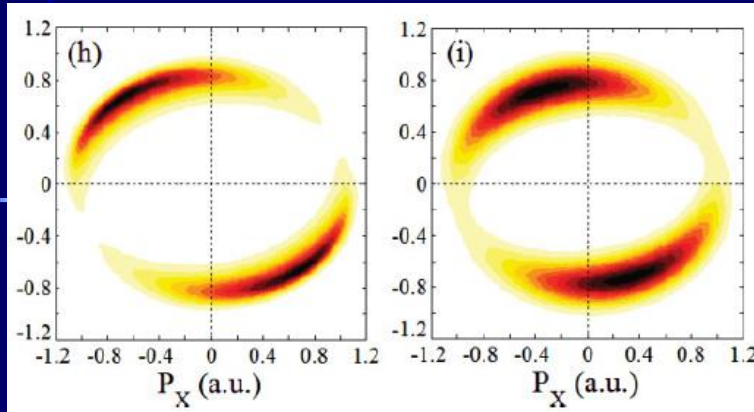
Mg
 $3.0 \times 10^{13} \text{ W/cm}^2$

Ca
 $3.0 \times 10^{13} \text{ W/cm}^2$

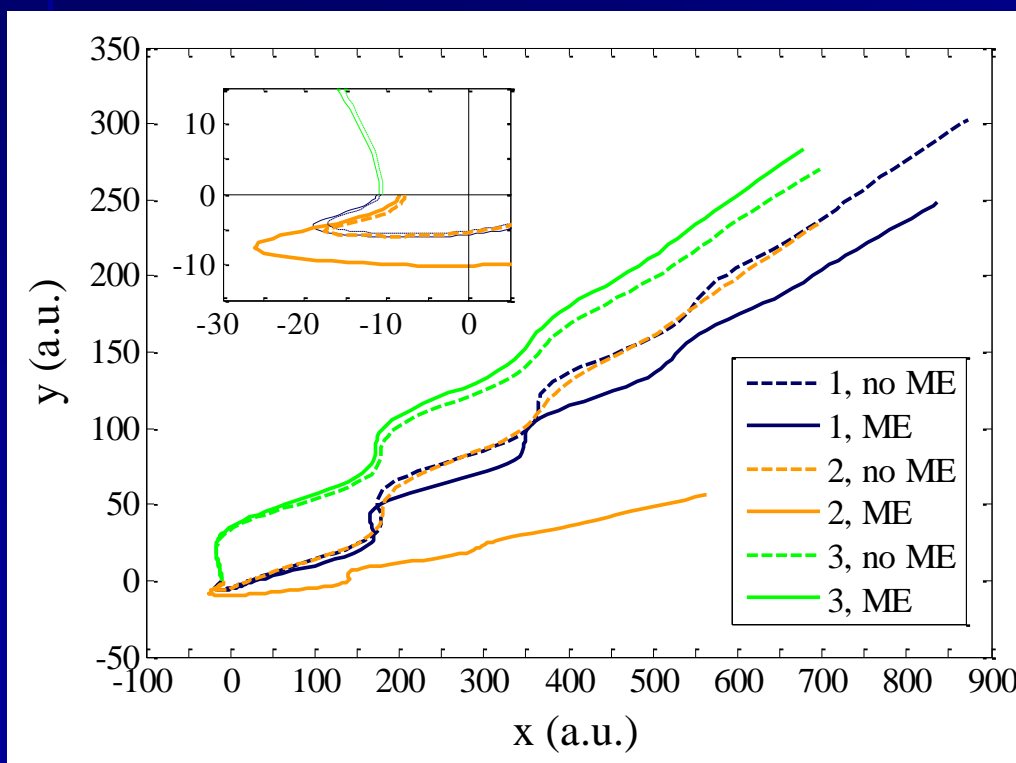
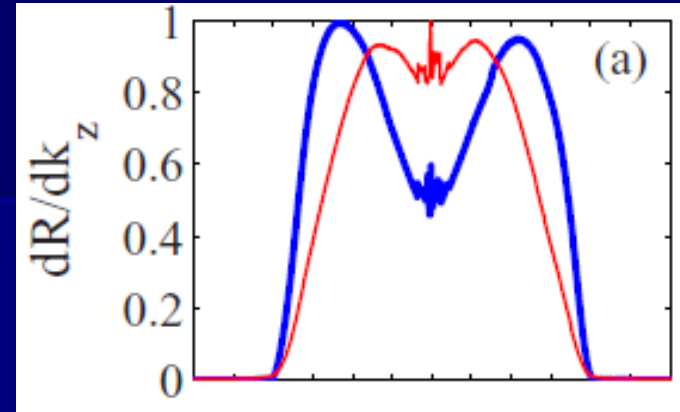
Modified from Fig. 3. in N. I. Shvetsov-Shilovski, M. Lein, and L. B. Madsen, Phys. Rev. A 98, 023406 (2018)

MULTELECTRON POLARIZATION EFFECTS

ellipticity = 0.78



linear polarization



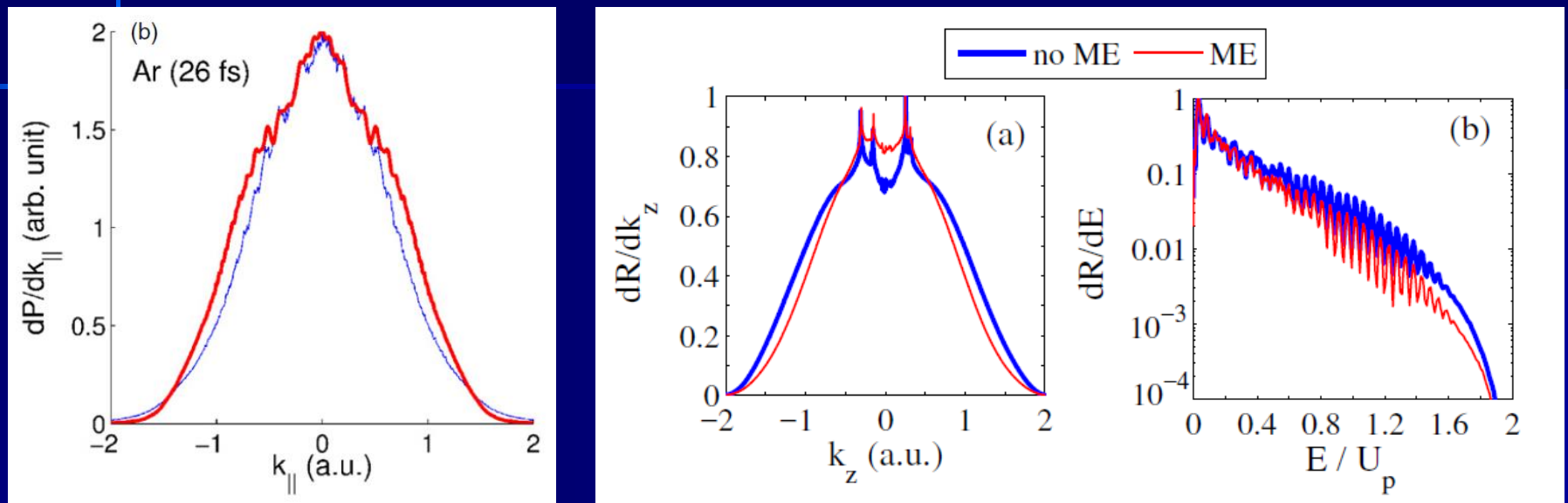
Three characteristic electron trajectories leading *in the absence of the ME potential* to the same final momentum
 $\vec{k}_0 = (0.86, 0.31)$ a.u.

3.0×10^{13} W/cm², 1600 nm,
8 cycles

MULTELECTRON POLARIZATION EFFECTS

A. Rudenko *et al.*, *J. Phys. B* 37, L407 (2004)

Ar, 800 nm, 4.0×10^{14} W/cm², 26 fs



Modified from Fig. 3 in M. Abu-Samha and L. B. Madsen, *J. Phys. B* 44, 253601 (2011)

Present simulations

The polarization effects may be important in resolving the remaining subtle discrepancy between the experiment and theory

Focal averaging ?

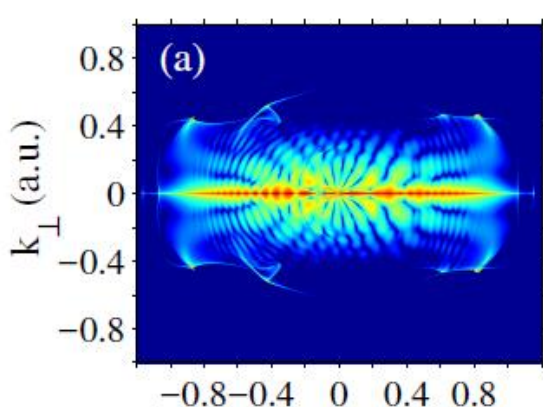
Laser-driven recollisions under the Coulomb barrier ?

Th. Keil, S. V. Popruzhenko, and D. Bauer, Phys. Rev. Lett., 117, 243003 (2016)

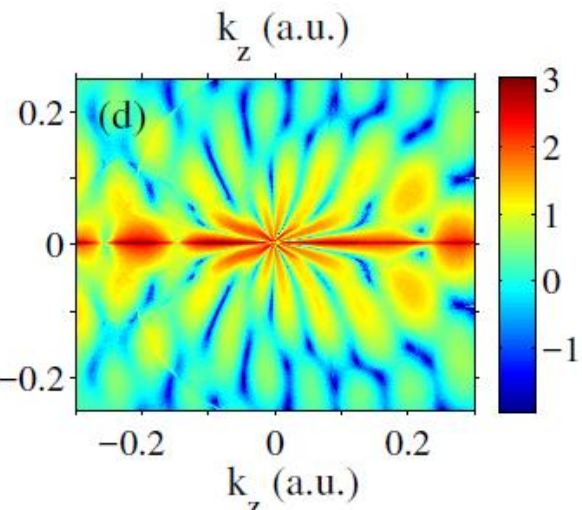
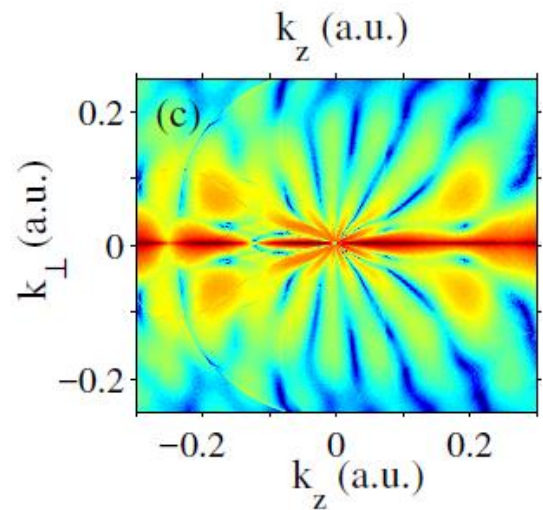
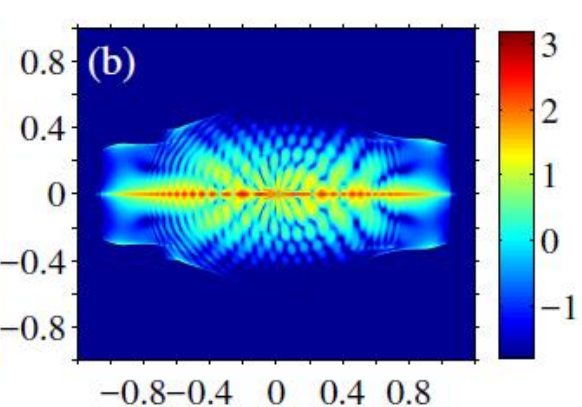
MULTELECTRON POLARIZATION EFFECTS

Polarization induced modification of interference patterns

No ME term in the phase



ME term in the phase



Ba, 3.0×10^{13} W/cm²,
1600 nm, 4 cycles

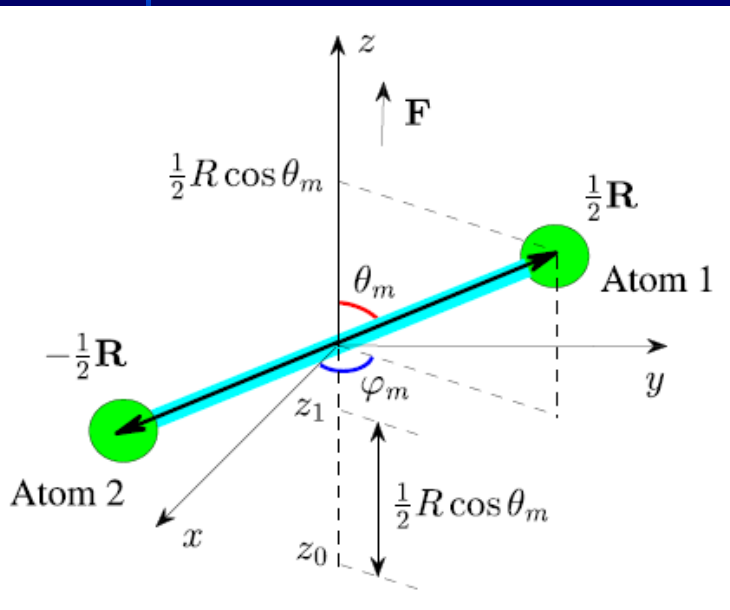
For both distributions the ME force is included in the equation of motion.

The number of fanlike interference structures for $|\vec{k}| < 0.25$ a.u. is different in the distributions calculated without and with the ME term in the phase.

STRONG-FIELD IONIZATION OF THE H₂ MOLECULE

$$V = -\frac{Z_1}{|\vec{r} - \vec{R}/2|} - \frac{Z_2}{|\vec{r} + \vec{R}/2|} \quad \text{H}_2^+ \quad Z_1 = Z_2 = 1/2$$

$$\frac{d^2\vec{r}}{dt^2} = -\vec{F}(t) - \frac{\vec{r} - \vec{R}/2}{2|\vec{r} - \vec{R}/2|^3} + \frac{\vec{r} + \vec{R}/2}{2|\vec{r} + \vec{R}/2|^3}$$



Partial Fourier transform for molecules

R. Murray, M. Spanner, S. Patschkoovskii,

*Phys. Rev. A **106**, 173001 (2011)*

*M. M. Liu and Y. Q. Liu, Phys. Rev. A **93**, 043426 (2016)*

Triangular barrier: $r_0 = -\frac{I_p}{F(t)}$

Field direction model (FDM):

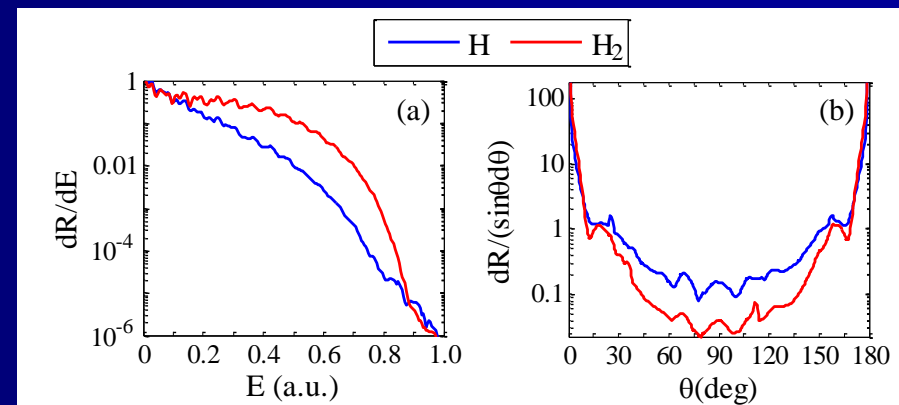
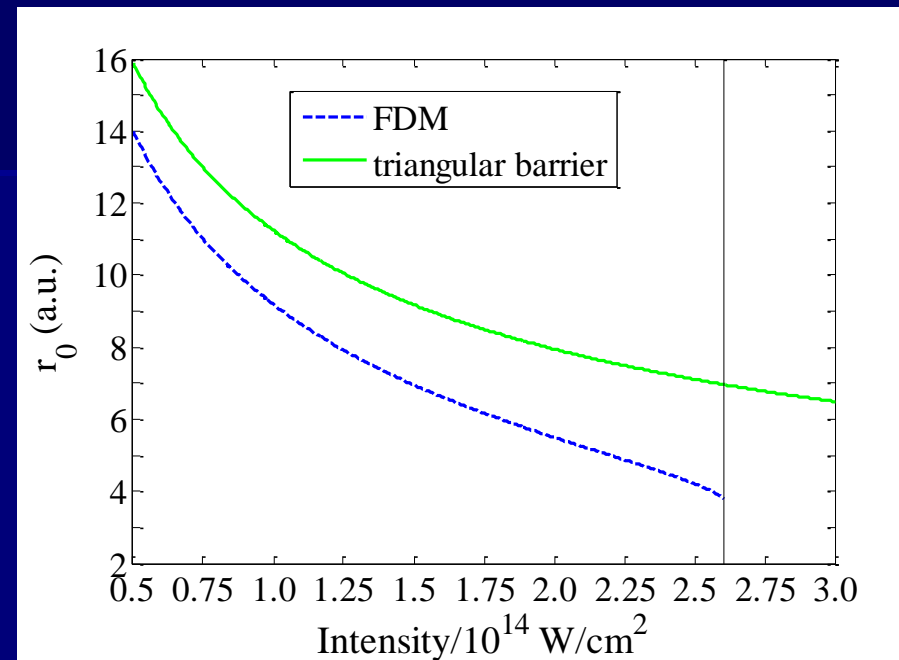
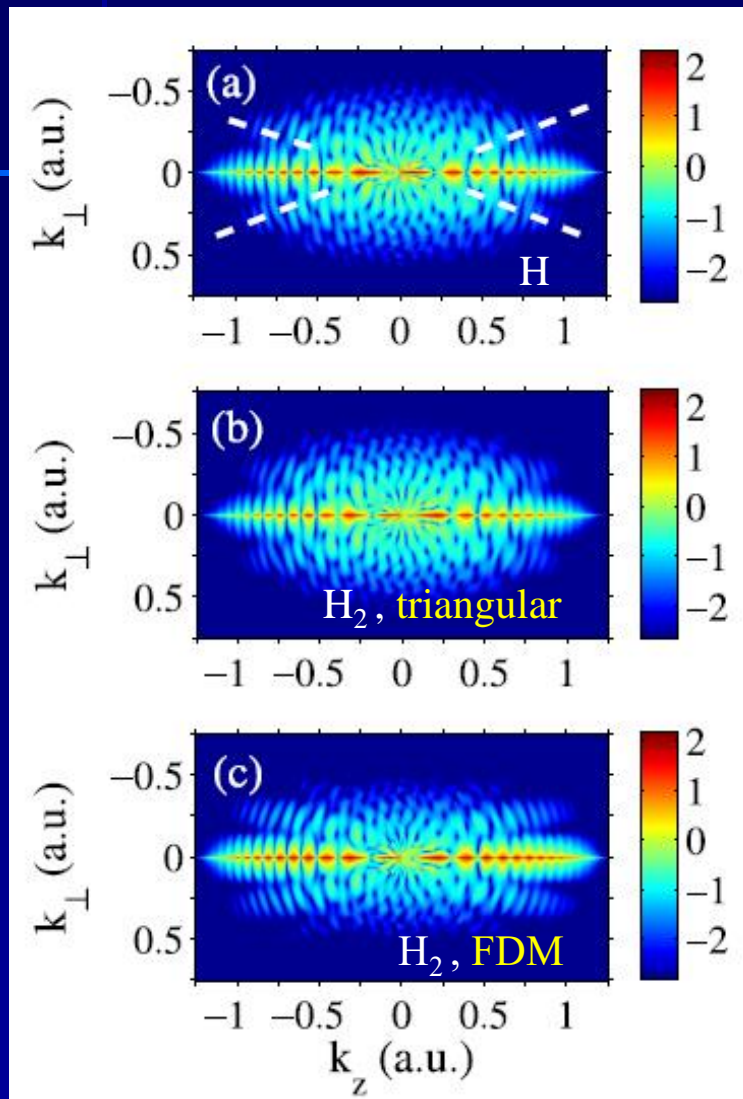
$$V(\vec{r}_0) + F(t_0)z_e = -I_p$$

$$S(t_0, v_0) = -\vec{v}_o \cdot \vec{r}(t_0) + I_p t_0$$

$$-\int_{t_0}^{\infty} dt \left\{ \frac{p^2(t)}{2} - \frac{Z_1(\vec{r} - \vec{R}/2) \cdot (2\vec{r} - \vec{R}/2)}{|\vec{r} - \vec{R}/2|^3} - \frac{Z_2(\vec{r} + \vec{R}/2) \cdot (2\vec{r} + \vec{R}/2)}{|\vec{r} + \vec{R}/2|^3} \right\}$$

STRONG-FIELD IONIZATION OF THE H₂ MOLECULE

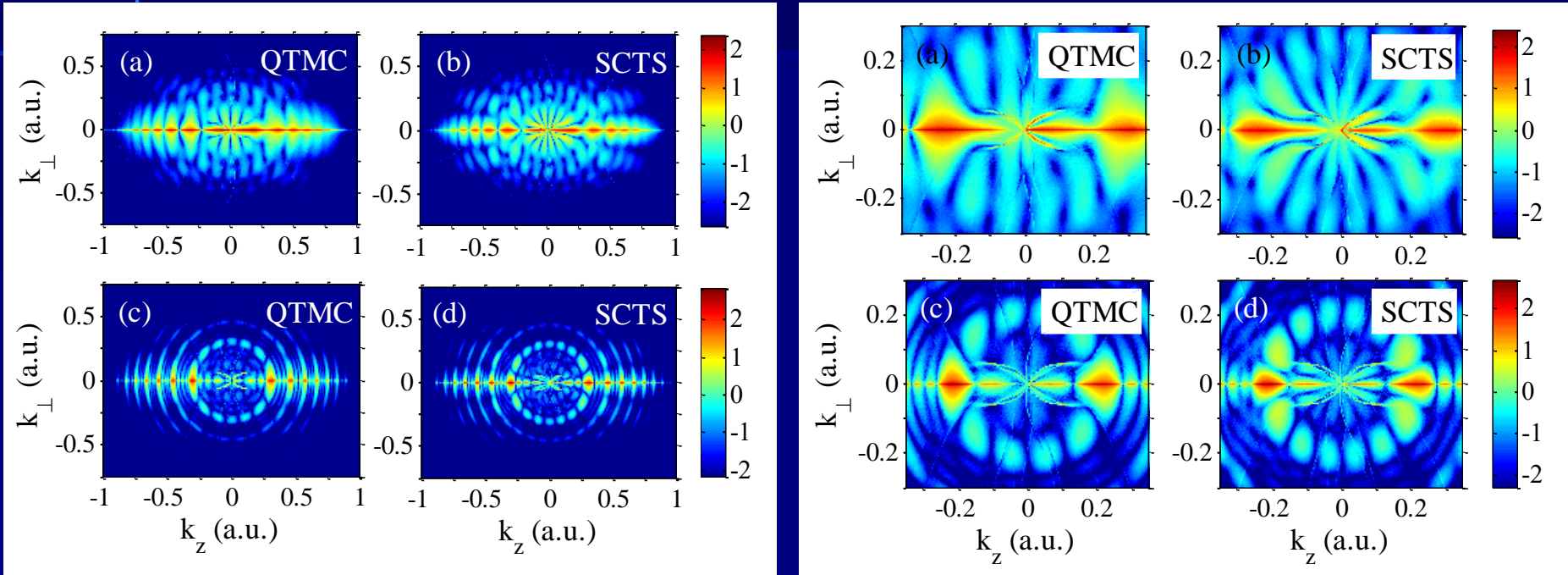
H and H₂, 3.0×10^{13} W/cm², 800 nm, 8 cycles



STRONG-FIELD IONIZATION OF THE H₂ MOLECULE

Comparison of QTMC and SCTS

H₂, 1.2×10¹⁴ W/cm², 800 nm, 8 cycles



Similar to the atomic case the QTMC predicts for H₂ molecule fewer nodal lines in the low-energy interference structure than the SCTS model

SEMICLASSICAL TWO-STEP MODEL WITH QUANTUM INPUT (SCTSQUI)

Quantum input:

- Starting point of the trajectory ?
- Initial velocity ?

$$\boxed{\frac{d^2\vec{r}}{dt^2} = -\vec{F}(t) - \nabla V}$$

Heisenberg's uncertainty principle: $\Delta x \cdot \Delta p_x \geq \frac{\hbar}{2}$ $\Psi(x, t)$  (x_0, p_x)

SFA formulas:

- T.-M. Yan, S. V. Popruzhenko, M. J. J. Vrakking, and D. Bauer, Phys. Rev. Lett. **105**, 253002 (2010)*
*R. Boge, C. Cirelli, A. S. Landsman et al., Phys. Rev. Lett. **111**, 103003 (2013)*
*J.-W. Geng, L. Qin, M. Li et al., J. Phys. B **47**, 204027 (2014)*

Backpropagation method:

- H. Ni, U. Saalmann, and J.-M. Rost Phys. Rev. Lett. **117**, 023002 (2016)*
*H. Ni, U. Saalmann, and J.-M. Rost, Phys. Rev. A **97**, 013426 (2018)*

Extended virtual detector theory:

- X. Wang, J. Tian, and J. H. Eberly, Phys. Rev. Lett. **110**, 243001 (2013)*
*X. Wang, J. Tian, and J. H. Eberly, J. Phys. B **51**, 084002 (2018)*
R.-H. Xu, X. Wang, and J. H. Eberly, arXiv:2003.05051 (2020)

SEMICLASSICAL TWO-STEP MODEL WITH QUANTUM INPUT (SCTSQUI)

$$i \frac{\partial}{\partial t} \Psi(x, t) = \left\{ -\frac{1}{2} \left(-i \frac{\partial}{\partial x} + A_x(t) \right)^2 - \frac{1}{\sqrt{x^2 + a^2}} \right\} \Psi(x, t)$$

TDSE + absorbing mask $M(x)$: $\tilde{\Psi}(x', t) = [1 - M(x)]\Psi(x, t)$

Gabor transformation:

$$G(x_0, p_x, t) = \frac{1}{\sqrt{2\pi}} \int_{-\infty}^{\infty} \tilde{\Psi}(x', t) \exp\left[-\frac{(x' - x_0)^2}{2\delta_0^2}\right] \exp(-ip_x x') dx'$$

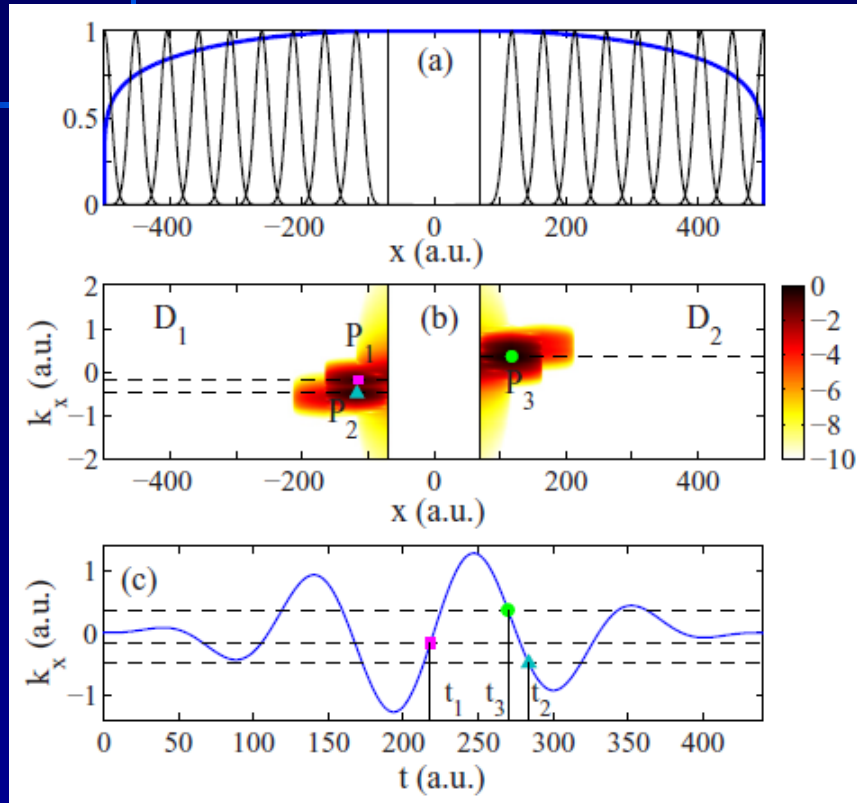
SCTSQUI:

$$R(k_x) = \left| \sum_{m=1}^{N_T} \sum_{j=1}^{n_{k_x}} G\left(t_0^m, x_0^j, p_{x,0}^j\right) \exp\left[i\Phi\left(t_0^m, x_0^j, p_{x,0}^j\right)\right] \right|^2$$

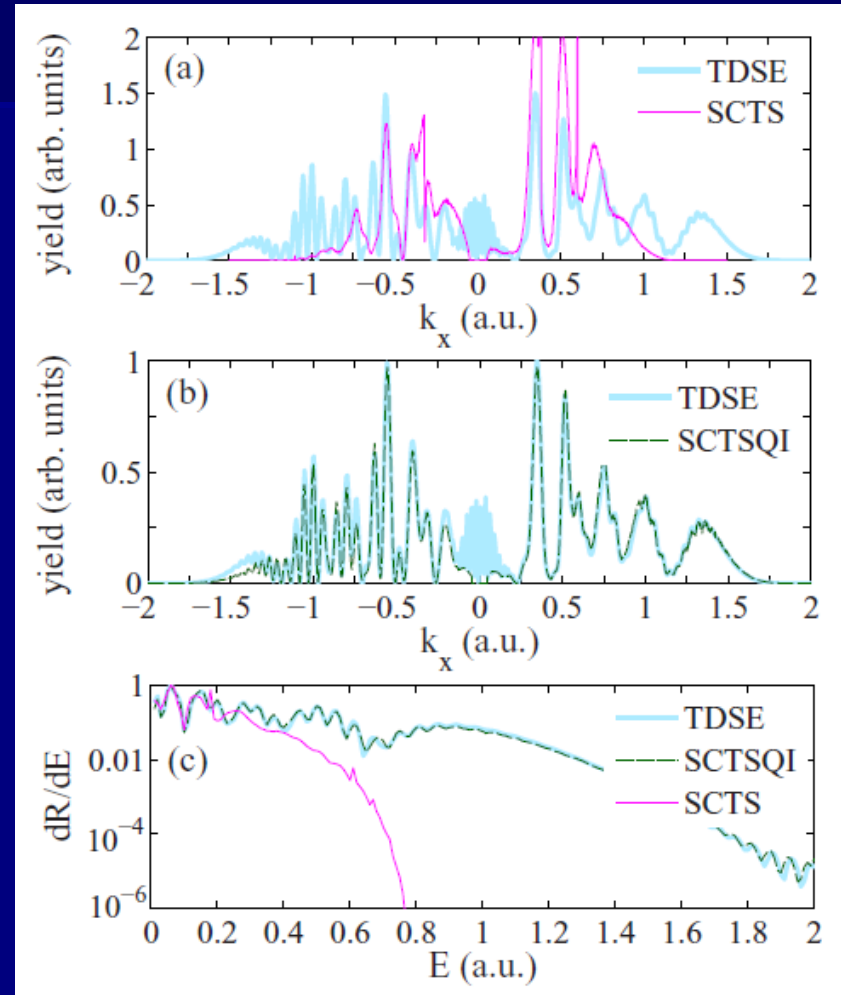
$$\Phi\left(t_0, x_0^j, p_{x,0}^j\right) = - \int_{t_0}^{\infty} dt \left\{ \frac{v_x^2(t)}{2} - \frac{x^2}{(x^2 + a^2)^2} - \frac{1}{\sqrt{x^2 + a^2}} \right\}$$

SEMICLASSICAL TWO-STEP MODEL WITH QUANTUM INPUT (SCTSQUI)

$2.0 \times 10^{14} \text{ W/cm}^2$, 800 nm, 4 cycles



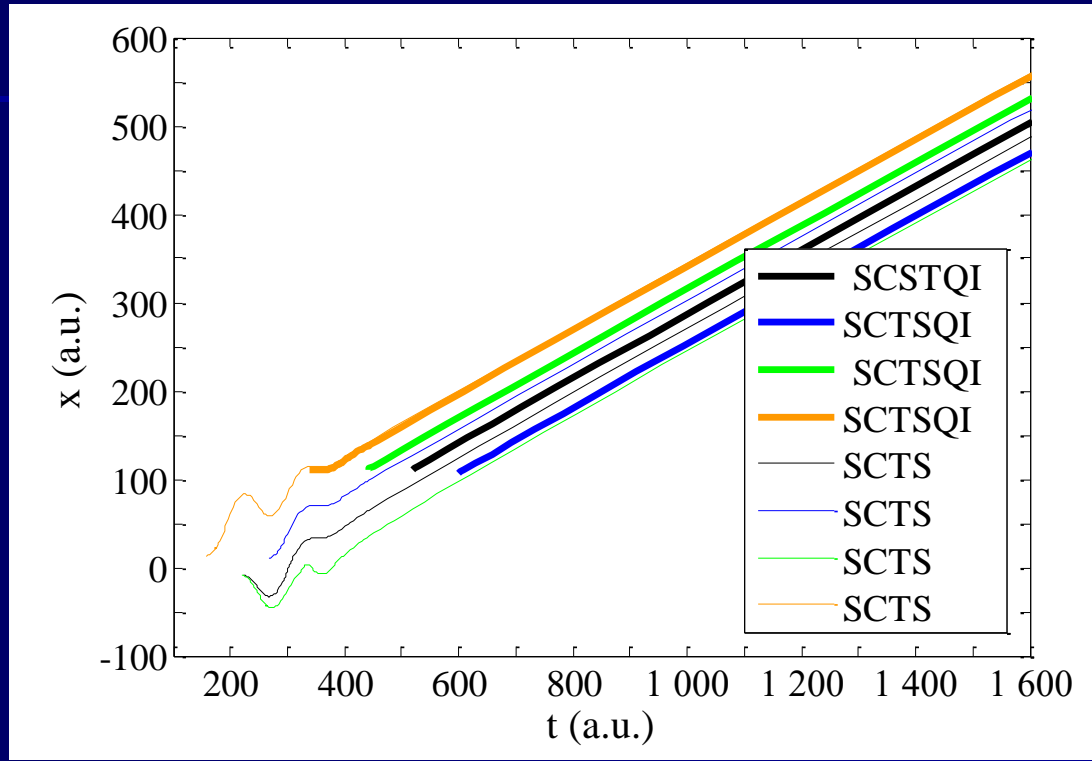
Modified from Figs 1 and 2 in
N. I. Shvetsov-Shilovski and M. Lein,
Phys. Rev. A **100**, 053411 (2019)



The SCTSQUI model yields **quantitative agreement** with the fully quantum results.

SEMICLASSICAL TWO-STEP MODEL WITH QUANTUM INPUT (SCTSQUI)

$2.0 \times 10^{14} \text{ W/cm}^2$, 800 nm, 4 cycles $k_x = 0.35 \text{ a.u.}$



The characteristic trajectories are different in the two models. We can expect the SCTSQI model provides a more accurate trajectory-based picture of the formation of the momentum distribution. The advantage of the SCTSQI approach should be used in the future for the analysis of more complex strong-field processes.

CONCLUSIONS

- Using the SCTS model we investigate the interference structures emerging in strong-field photoelectron holography, taking into account the Coulomb potential of the atomic core. For every kind of the interference pattern predicted by the three-step model, we calculate the corresponding structure in the presence of the Coulomb field, showing that the Coulomb potential modifies the interference patterns significantly.
- We extend the SCTS model to include polarization-induced dipole potential. We predict a pronounced narrowing of the photoelectron momentum distributions in the longitudinal direction parallel with the laser polarization. The narrowing is caused by the polarization-induced dipole force on electrons that start relatively close to the origin. Polarization of the core also modifies interference structures.
- We extend the SCTS model to the hydrogen molecule. We predict significant deviations of the two-dimensional photoelectron momentum distributions and the energy spectra from the case of atomic hydrogen.
- We develop a mixed quantum-classical approach to strong-field ionization – a semiclassical two-step model with quantum input (SCTS_{QI}). In the SCTS_{QI} the initial conditions for classical trajectories are determined by the exact quantum dynamics. For ionization of a one-dimensional atom the model yields quantitative agreement with the quantum result.